TÜBİTAK

Turkish Journal of Engineering & Environmental Sciences

http://journals.tubitak.gov.tr/engineering/

Research Article

Turkish J Eng Env Sci
(2013) 37: 42 – 55

doi:10.3906/muh-1109-9

Exergetic evaluation of an integrated gasification combined cycle power plant simulated by seven different types of Turkish lignite

Ehsan AMIRABEDIN, Mustafa Zeki YILMAZOĞLU*, Şenol BAŞKAYA
Department of Mechanical Engineering, Faculty of Engineering, Gazi University,
06570 Maltepe, Ankara, Turkey

Received: 20.09.2011 • **Accepted:** 19.09.2012 • **Published Online:** 04.03.2013 • **Printed:** 01.04.2013

Abstract: In this study, exergy analysis of an integrated gasification combined cycle (IGCC) operating with 7 different types of low rank Turkish lignite was performed. The purpose was to determine and compare the performance of each type of lignite in the same gasifier. Exergy destruction of each component and exergetic performance of the overall plant was also investigated. In addition, CO_2 emissions of each type of lignite were calculated. The results showed that Yeniköy lignite had the best performance among the different types of lignite, with 491 MW net power and 37.88% net exergy efficiency (without acid gas). It also had the minimum amount of CO_2 emission at 726 kg/MWh. Therefore, Yeniköy lignite was chosen as a case study fuel and a detailed exergy analysis of its components was applied. The results showed that the major exergy destructions took place in the gasifier and the combustion chamber at 46.15% and 22.74%, respectively.

Key words: Integrated gasification combined cycle, exergy analysis, low rank Turkish lignite, CO_2 emissions

1. Introduction

Coal is the most abundant and vital energy source for energy conversion systems. Primary energy requirements, electricity generation, steel production, and other industrial sectors widely use coal as an energy source due to low price and higher abundance. As a result of coal combustion, CO_2, SO_2, NO_x, fly ash, dust, and other emissions are released to the atmosphere. As reported by the International Energy Agency, Turkey generates 27% of total electricity production from coal, which shows a growing trend due to increasing natural gas prices. Moreover, between the years 2001 and 2008 for Turkey, 0.429 and 0.558 kg of CO_2 was released into the atmosphere per kWh of electricity generation (Ari and Koksal, 2011). As a well-known fact, CO_2 emissions in the atmosphere contribute to global warming with greenhouse gas effects.

Clean coal technologies have an increasing trend and utilize coal very efficiently without harmful effects. The most promising technology for effective and harmless utilization of coal is gasification. An integrated gasification combined cycle (IGCC) uses coal to produce hydrogen and CO in a gasifier, and combustion takes place in the combustion chamber of a gas turbine. It has advantages and disadvantages when compared to other alternatives. The net efficiency of an IGCC is larger compared to a conventional thermal power plant and less than a natural gas fired combined cycle. It depends on the gasification and gas cleaning technology. Gasifier type, oxidant type, coal feeding system, and gas cleaning system selections directly affect the performance of

*Correspondence: zekiyilmazoglu@gazi.edu.tr

the overall power plant. Jiang et al. (2002) performed an optimization study on the steam side of an IGCC and the effects of this optimization on the net efficiency were given. According to the results of that study, increasing the gas turbine (GT) outlet temperature increases the net efficiency, and in the case of 10 °C pinch point temperature for the evaporator of the heat recovery steam generator (HRSG), the efficiency was found to be the highest. They also showed the effects of GT outlet temperature on the bottoming cycle efficiency; at 600 °C outlet temperature, the efficiency of the bottoming cycle with a single and dual pressure HRSG was found to be 38% and 40%, respectively. At this temperature the ratio of steam turbine output to the gas turbine output was 63% for a dual pressure HRSG. Fortes et al. (2009) compared 8 different types of feedstock in an IGCC power plant with ASPEN software using real plant data sets. Co-gasification of coal with pet coke and olive pomace was performed. According to the results of their simulation, coal shows the best efficiency when compared to other alternatives and the efficiency of the overall power plant was found to be 52%. Huang et al. (2008) simulated 2 alternatives of an IGCC with 6 cases using ECLIPSE software. The efficiency penalty for CO_2 capture was approximately 8% to 10% of the total efficiency. The cost of CO_2 capture was found as US$22/t CO_2, and economic analysis of CO_2 transportation was also performed. Zheng and Furinsky (2005) compared different types of gasifiers for 3 different fuel stocks using ASPEN PLUS software. Heating values of clean syngas, compositions of syngas, and power plant parameters were compared, and they indicated that lignite is the best fuel feedstock when compared to subbituminous and bituminous coals. The variation of thermal efficiency was found to be less than 0.5% with respect to coal type and KRW type of gasifier. Garcia et al. (2006) performed a case study by using ASPEN PLUS software and compared the CO_2 capture costs of different simulated cases. CO_2 capture cost varied between $28/t and 30/t CO_2, depending on the CO_2 capture efficiency. Duan et al. (2004) suggested a novel cycle with semiclosed Brayton cycle and steam injected H_2/O_2 cycle to capture CO_2 more effectively. Rezenbrink et al. (2009) reported a 450 MW IGCC/CCS project and made an economic analysis for CO_2 avoidance and storage costs. The expected efficiency and specific CO_2 emissions of the IGCC were 34% (LHV) and 107 g/kWh net. Jimenez et al. (2010) performed a simulation using ASPEN PLUS software. The Texaco gasifier was selected as the base case and the efficiency of the cycle was found to be 45% (LHV). The results showed that CO_2 and SOx emissions can be reduced to 698 kg/MWh and 0.15 kg/MWh, respectively. Chen and Rubin (2009) analyzed CO_2 capture costs for different types of coals in an IGCC. ASPEN PLUS was used for the simulations and GE type Quench gasifier was selected. CO_2 capture (CCS) was obtained by the Selexol process. According to the results of their simulations, CCS reduces the power plant efficiency by 10%–16%, and the first investment cost of the power plant increases by 23%–27%. The minimum cost of electricity generated in an IGCC was found to be $80.4/MWh at 2008 prices, where ion transport membrane and a H type gas turbine were used in the simulations. Decamps et al. (2008) showed the effects of CO_2 capture on IGCC performance and the results showed that IGCC efficiency decreased with CCS by 8%–12% when compared to a non-CCS IGCC power plant. Mondol et al. (2009) simulated a novel IGCC-CCS power plant in ECLIPSE and compared the results with those for IGCC power plants with and without CCS. The absorption enhanced reforming process was used for CO_2 capture and a hot gas cleaning system was offered. The results showed that the proposed CO_2 capture plant efficiencies are between 18.5% and 21% compared to a conventional IGCC CO_2 capture plant. The specific investment cost of proposed power plants were between 1207 and € 1493/kWe.

The aim of this study was to simulate an IGCC by utilizing the THERMOFLEX simulation software. In addition, an exergy analysis was performed based on the second law of thermodynamics in order to evaluate the exergy efficiency and exergy destruction of the overall power plant and each of its components. Thus, the

extent and exact location of the exergy destruction in the system was identified. A GE (Texaco) type gasifier with one stage, slurry fed, oxygen blown, and a cold gas cleaning system was considered for the simulations. Yeniköy lignite was chosen as the case study fuel. In addition, the simulated IGCC was operated with 6 other types of Turkish lignites that are currently being employed in thermal power plants in Turkey. The results were compared in terms of power generation, exergy efficiency, and CO_2 emissions for each type of lignite.

2. Description of the power plant

A basic schematic diagram of an IGCC with GE gasifier is illustrated in Figure 1. In this type of gasifier, lignite is fed into the gasifier as wet slurry. This wet slurry is mixed with high pressure and high temperature water, which is provided from a HRSG and finally pumped to the gasifier. Therefore, higher operating pressures at the gasifier can be achieved. Oxygen from an air separation unit is blown into the gasification reactor. Operating temperature and pressure of the gasifier are 1320 °C and 33 bar, respectively. Most of the ash is removed as solid slag at the base of the reactor. For the cold cleaning process, produced raw syngas is cooled in a radiant cooler, which is situated directly below the gasifier reactor. This cooler provides evaporation heating of the high pressure steam. The cooled raw syngas exits the gasifier vessel and enters a wet-scrubber. Fly ash and any HCL are absorbed in this component. Following it, a COS hydrolysis reactor converts COS to H_2S. H_2S is then removed from the syngas by an acid gas remover. COS hydrolysis and acid gas removal are used together to reduce plant sulfur emissions, potential for fouling and corrosion, in the HRSG. In the COS hydrolysis plant the syngas passes through a catalyst where COS reacts with water vapor in the syngas to produce H_2S and CO_2. The reaction is given in Eq. (1).

$$COS + H_2O \rightarrow H_2S + CO_2 \tag{1}$$

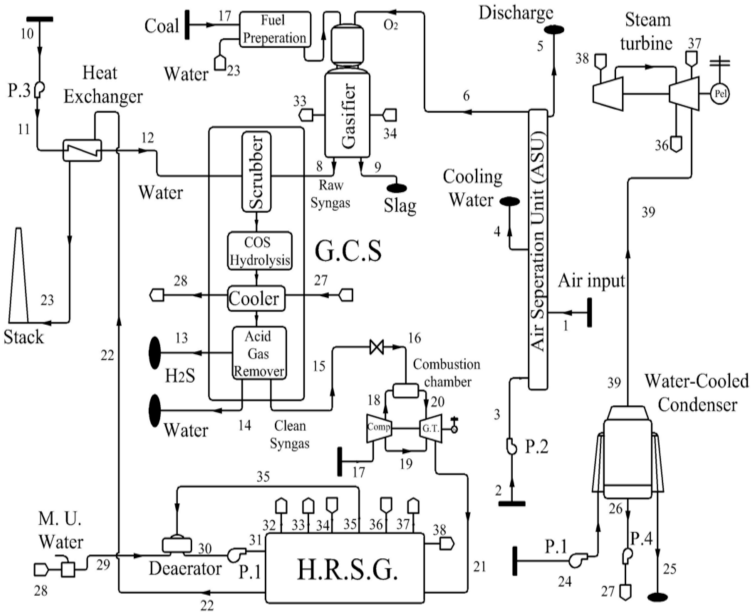

Figure 1. Schematic diagram of the IGCC (gasifier type: Texaco).

The pressure of the clean syngas should be higher than the pressure of the combustion chamber of the gas turbine. However, in this IGCC plant the pressure of the syngas is much greater than that of the combustion chamber pressure. In order to reduce the pressure of the syngas, a valve is installed just before the gas turbine. The clean syngas is then delivered to the Mitsubishi 701F model gas turbine-generator with 315 MW electrical power (in ISO condition). Exhaust gases from the gas turbine are passed to the HRSG, supplying the steam to generate additional electricity through a steam turbine.

The cooled combustion gas is used in a heat exchanger to heat the scrubber water. After that, it is exhausted via the stack to the atmosphere. The expanded steam, leaving the steam turbine, is pumped by the condensate extraction pump to the integral deaerator. The high pressure pump forces the condensate through the HRSG and completes the steam cycle.

3. Exergy analysis

The exergy of a system is defined as the maximum available work that can be done by the system–environment combination. A higher value of exergy means a higher value of obtainable work. The exergy analysis is the composite of the first and second laws of thermodynamics.

In this analysis, heat does not have the same value as work, and exergy loss represents real loss of work. When analyzing novel and complex thermal systems, experience needs to be supplemented by more rigorous quantitative analytical tools. Exergy analysis provides those tools and helps in locating weak spots in a process. This analysis provides a quantitative measure of the quality of the energy in terms of its ability to perform work and leads to a more rational use of energy (Oktay, 2009).

For a real process, the exergy input always exceeds the exergy output; this unbalance is due to irreversibilities, which are known as exergy destruction (Dincer and Al-Muslim, 2001).

The general form of the exergy equation for an open system control volume is given in Eq. (2) (Bejan, 1988, 1996).

$$\frac{dE_{cv}}{dt} = \sum_j \left(1 - \frac{T_0}{T_i}\right)\dot{Q}_j - \left(\dot{W}_{cv} - p_0\frac{dV_{cv}}{dt}\right) + \sum_i \dot{m}_i e_i - \sum_e \dot{m}_e e_e - \dot{E}_D \tag{2}$$

The exergy equation for the system at steady state conditions is given in Eq. (3), where time rate variations given in Eq. (2) are neglected.

$$0 = \sum_j \left(1 - \frac{T_0}{T_i}\right)\dot{Q}_j - \left(\dot{W}_{cv}\right) + \sum_i \dot{m}_i e_i - \sum_e \dot{m}_e e_e - \dot{E}_D \tag{3}$$

Rearranging Eq. (3) gives the exergy destruction of a steady state open system for a control volume.

$$\dot{E}_D = \sum_j \dot{E}_{qj}\dot{Q}_j - \left(\dot{W}_{cv}\right) + \sum_i \dot{E}_i - \sum_e \dot{E}_e \tag{4}$$

It must be noted that, in this study, the exergy destructions caused by the heat losses from the components in the first term of Eq. (4) are neglected, since it has been assumed that the boundary temperature of each component due to ideal insulation (T_j) is equal to the ambient temperature (T_0). Therefore:

$$\dot{E}_D = -\left(\dot{W}_{cv}\right) + \sum_i \dot{E}_i - \sum_e \dot{E}_e. \tag{5}$$

In the absence of nuclear, magnetic, electrical, and surface tension effects, the total exergy of a system $\dot{E}$ can be divided into 4 components.

$$\dot{E} = \dot{E}_{PH} + \dot{E}_{CH} + \dot{E}_{PT} + \dot{E}_{KN} \tag{6}$$

By neglecting potential and kinetic energy, Eq. (6) can be rewritten as indicated in Eq. (7).

$$\dot{E} = \dot{E}_{PH} + \dot{E}_{CH} \tag{7}$$

The specific physical exergy (e_{PH}) can be expressed as follows, where subscript "0" indicates reference conditions.

$$e_{PH} = h - h_0 - T_0 (s - s_0) \tag{8}$$

The total exergy rate ($\dot{E}$) can be written as a function of mass flow rate ($\dot{m}$) and specific physical and chemical exergies, and is given in Eq. (9).

$$\dot{E} = \dot{m} [h - h_0 - T_0 (s - s_0) + \bar{e}_{CH}] \tag{9}$$

The molar specific chemical exergy ($\bar{e}_{CH}$) of a substance can be obtained from standard chemical exergy tables (Kotas, 1985) relative to specification of the environment. For mixtures containing gases other than those present in the reference tables, molar chemical exergy can be evaluated with Eq. (10).

$$\bar{e}_{CH} = \sum x_n (\bar{e}_{CH})_n + \bar{R} T_0 \sum x_n \ln x_n \tag{10}$$

In Eq. (10), x_n is the mol fraction of the k_{th} gas in the mixture and $\bar{R}$ is the universal gas constant.

A procedure for the determination of the chemical exergy based on stoichiometric combustion of coal was developed by Bejan (1998). In this study, for the calculation of the specific chemical exergy of Turkish lignites, the same method was utilized. On the basis of 1 kg of dry and ash free (DAF) lignite entering the boiler, the combustion reaction is described as follows.

$$(cC + hH + oO + nN + sS) + v_{O_2} O_2 \rightarrow v_{CO_2} CO_2 + v_{H_2O} H_2O(l) + v_{SO_2} SO_2 + v_{N_2} N_2 \tag{11}$$

Parameters v of the molar mass balance of the combustion reaction without oxidation of nitrogen can be obtained by the following equations.

$$v_{CO_2} = c \quad v_{H_2O} = \frac{1}{2} h \quad v_{SO_2} = s$$

$$v_{N_2} = \frac{1}{2} n \quad v_{O_2} = c + \frac{1}{4} h + s - \frac{1}{2} o \tag{12}$$

Chemical exergy of the DAF lignite (e^{CH}_{DAF}) can be described as a function of the DAF higher heating value $(HHV)_{DAF}$, the specific absolute entropy of DAF lignite (s_{DAF}), the molar entropy ($\bar{s}$), the molar chemical exergies of the lignite ingredients ($\bar{e}^{CH}$), and the ambient temperature (T_0). As a result, we have the following.

$$\begin{aligned} e^{CH}_{DAF} = (HHV)_{DAF} - T_0 [s_{DAF} + v_{O_2} \bar{s}_{O_2} - v_{CO_2} \bar{s}_{CO_2} - v_{H_2O} \bar{s}_{H_2O} - v_{SO_2} \bar{s}_{SO_2} \\ - v_{N_2} \bar{s}_{N_2}] + [v_{CO_2} \bar{e}^{CH}_{CO_2} + v_{H_2O} \bar{e}^{CH}_{H_2O} + v_{SO_2} \bar{e}^{CH}_{SO_2} + v_{N_2} \bar{e}^{CH}_{N_2} - v_{O_2} \bar{e}^{CH}_{O_2}] \end{aligned} \tag{13}$$

A higher heating value of DAF lignite $(HHV)_{DAF}$ can be estimated as given below.

$$(HHV)_{DAF} = [152.19H + 98.767][(C/3) + H - (O - S)/8] \tag{14}$$

Here, C, H, O, and S are the mass fractions of the DAF lignite.

s_{DAF} is the specific absolute entropy for DAF lignite and can be estimated as given below.

$$s_{DAF} = c[37.1653 - 31.4767\exp(-0.5646\frac{h}{c+h}) + 20.1145\frac{o}{c+n} + 54.311\frac{n}{c+n} + 44.6712\frac{s}{c+n}] \quad (15)$$

Here, c, h, o, n, and s are the molar mass fractions of ingredients of the DAF lignite on a kmol/kg basis.

After the determination of the specific chemical exergy of DAF lignite, the specific exergy of raw lignite (as received) can be calculated by summing the chemical exergies of the DAF lignite and moisture content.

$$e^{CH}_{lignite} = m_{DAF}[\frac{kg(DAF)}{kg(Total)}]e^{CH}_{DAF} + m_l[\frac{kg(H_2O)}{kg(Total)}]e^{CH}_{H_2O} \quad (16)$$

Here, m_{DAF} is the mass fraction of the DAF lignite and m_l is the mass fraction of the water content of the raw lignite.

In the exergy analyses, another significant matter that must be presented is the reference condition. In this study, the atmospheric temperature and pressure were taken as reference conditions: 25 °C and 101.32 kPa, respectively.

Another parameter in the exergy analysis of a system is the exergy efficiency, which is the percentage of the exergy of the product (desired output) over the fuel exergy provided to a system. Here, fuel exergy in general means is defined as the entire resources supplied to the system (e.g., fuel, air, water). Considering this fact, the desired outcome and the given resource of the different components of the power plant can have different definitions.

However, second law energy efficiency (exergy efficiency), ε, can be expressed as:

$$\varepsilon = \frac{\dot{E}_P}{\dot{E}_F}. \quad (17)$$

Further expressions and efficiencies of the exergy of each component of the investigated power plant are summarized in the Appendix.

4. Results

4.1. Simulation results of the IGCC operating with Yeniköy lignite

The general performance of the simulated power plant is given in Table 1. In addition, according to the supplementary simulation results, the raw syngas enters the radiant cooler with a pressure of 32.52 bar and temperature of 1371 °C. The pressure drop at the radiant syngas cooler section is calculated as 1.626 bar. The exit temperature and pressure of the syngas are 732 °C and 30.89 bar, respectively. Total heat transfer to the water wall is calculated to be 137.634 MW. Moreover, the exit pressure and temperature from the convective syngas cooler is found to be 28.22 bar and 197.8 °C, respectively. Table 2 shows the raw and clean syngas compositions.

Table 1. IGCC summery.

Characteristic	Unit	Value
Gross power	MW	528.18
Net power (electricity production)	MW	491.02
Generated power via gas turbine	MW	613.40
Generated power via steam turbine	MW	216.95
Compressor power input	MW	293.68
Total plant auxiliary	MW	37.15
Total fuel consumption	kg/s	76.00
Net energy efficiency	%	44.17
Plant total CO_2 emission	kg/h	383440
Plant total SO_2 emission	kg/h	84.19

Table 2. Raw and clean syngas compositions by volume.

	CO	CO_2	CH_4	H_2	H_2S	H_2O	COS	N_2
Raw Syngas	30.22	13.53	0.002	22.75	0.58	31.00	0.03	1.89
Clean Syngas	44.06	19.76	0.003	33.17	0.001	0.23	0.001	2.76

The lower heating value of the raw syngas is calculated to be 6783 kJ/kg. After the cleaning process, the volume percentage of CO and H_2 increases and the lower heating value of the clean syngas becomes 9106 kJ/kg. Meanwhile, at the exit of the oxygen compressor, the pressure of oxygen is found to be 33 bar and the temperature of the oxygen is 120.4 °C. The mass flow rate of oxygen (95% purity) is 41.60 kg/s. The total shaft power of the syngas combusted at the gas turbine is 613.4 MW, and the exit temperature of the combustion gas is 595 °C. The temperature and the mass flow rate of the combustion gas affect the design of the HRSG. The combustion gases pass through the superheater, reheater, evaporator, and economizer packages, respectively. Steam is generated at a pressure of 116.7 bar. The temperature of the superheated steam is 521.5 °C. The condenser pressure is taken as 0.065 bar and the saturation temperature at this point is 37.6 °C. The rejected heat from the condenser is found to be 336 MW. The stack temperature and the mass flow rate of flue gas are 126 °C and 757.3 kg/s, respectively. The thermodynamic properties of each stream of the IGCC are presented in Table 3. Power consumption of the auxiliary devices of the IGCC are given in Table 4.

4.2. Exergy analysis results of the IGCC operated with Yeniköy lignite

The exergy analysis of the IGCC is accomplished with the equations given in Section 3. The physical, chemical, and total exergy rates of air, lignite, syngas, acid gas, combustion gases, steam, and water at various points are computed and summarized in Table 5. The chemical exergy of the air at points 1, 5, 17, 18, and 19 is assumed to be zero since the air composition at these points resembles the reference environment. In addition, the physical exergy of coal and slag are neglected due to ignorable changes of their entropies.

Table 6 provides a list of the exergy destruction and exergy efficiency data for various components of the IGCC. As is obvious here, the highest exergy destruction occurs in the gasifier and combustion chamber. The dimensionless exergy destructions (Coskun et al., 2011) of the gasifier and combustion chamber are calculated to be 46.24% and 25.93% of the total exergy destruction, respectively. The other prominent components in exergy destruction are the gas cleanup system, gas turbine, and steam turbine, respectively, with 11.97%, 5.47%, and 3.72% of total exergy destruction. In spite of the first law analysis indicating that the greatest exergy loss

Table 3. Thermodynamic properties of each stream of the power plant.

Point	State	T (°C)	P (kPa)	m (kg/s)	h (kJ/kg)	s (kJ/kg K)
1	A	25.0	101.3	173.2	–162.44	6.9534
2	W	25.0	101.3	376.9	104.85	0.3674
3	W	25.0	543.0	376.9	105.02	0.3670
4	W	35.0	470.1	376.9	146.76	0.5056
5	A	25.0	101.3	131.6	–162.45	6.9534
6	Oxyg	120.4	3300.0	41.6	89.01	5.8262
7	Coal	25.0	101.3	76.0	0.00	0.0000
8	Syng	732.2	3135.0	117.3	–6439.50	10.2040
9	Slg	100.0	3508.0	15.5	0.00	0.0000
10	W	25.0	101.3	44.3	104.85	0.3674
11	W	25.2	3358.0	44.3	105.72	0.3639
12	W	125.0	3135.0	44.3	524.98	1.5812
13	W	110.2	3157.0	75.0	462.41	1.4213
14	AcGs	37.8	3157.0	1.1	–589.05	5.2363
15	Syng	197.8	2822.0	85.5	–5392.19	8.3406
16	Syng	197.8	2550.0	85.5	–5392.19	8.3780
17	A	25.0	101.3	671.9	–162.45	6.9534
18	A	444.3	1872.0	585.6	279.88	7.0281
19	A	444.3	1872.0	86.3	279.88	7.0281
20	CG	1357.7	1797.0	671.0	–222.45	8.0409
21	CG	595.4	104	757.3	–1175.18	8.0641
22	CG	149.4	101.5	757.3	–1677.65	7.2639
23	CG	126.0	101.3	757.3	–1702.53	7.2041
24	W	25.0	101.3	8061.1	104.85	0.3674
25	W	35.0	101.3	8061.1	146.76	0.5046
26	W	37.6	42.4	150.8	157.69	0.5409
27	W	37.6	290.0	150.8	157.77	0.5405
28	W	131.7	290.0	150.8	553.62	1.6525
29	W	120.9	290.0	166.4	507.50	1.5372
30	W	132.4	339.1	170.2	556.48	1.6595
31	W	135.4	11,702.0	170.2	569.27	1.6800
32	W	321.6	11,690.0	15.2	1471.95	3.4649
33	W	321.6	11,690.0	112.5	1471.95	3.4649
34	S	322.6	11,690.0	112.5	2691.32	5.5111
35	S	322.6	11,690.0	3.8	2691.32	5.5111
36	S	338.0	3185.0	150.8	3081.53	6.6619
37	S	524.1	3060.0	150.8	3510.24	7.2908
38	S	519.7	11,500.0	150.8	3406.30	6.5806
39	S/W	37.6	6.5	150.8	2385.92	7.7103

Enthalpy and entropy are calculated from the methods of Bejan (1996).

A - air, W - water, Oxyg - oxygen, Syng - syngas, Slg - slag, AcGs - acid gas removal, CG - combustion gas, S - steam, S/W - steam–water mixture.

Table 4. Power consumption of auxiliary devices.

Component	W (MW)
W_{ASU}	20.3
$W_{Cond.P.}$	1.6
W_{GCS}	5.1
$W_{Gas.}$	6.0
$W_{P.1}$	3.7
$W_{P.2}$	0.2
$W_{P.3}$	0.2
$W_{P.4}$	0.06

Table 5. Physical, chemical, and total exergy of each stream.

Point	State	Physical (MW)	Chemical (MW)	Total (MW)
1	A	-	-	-
2	W	0.00	65.27	65.27
3	W	0.11	65.27	65.38
4	W	0.27	65.27	65.54
5	A	-	-	-
6	Oxyg	11.79	4.34	16.13
7	Coal	-	1296.37	1296.37
8	Syng	116.21	803.49	919.70
9	Slg	-	20.40	20.40
10	W	-	7.68	7.68
11	W	0.08	7.68	7.76
12	W	2.58	7.68	10.26
13	W	3.25	13.00	16.25
14	AcGs	0.28	26.80	27.09
15	Syng	35.79	765.30	801.09
16	Syng	34.83	765.30	800.13
17	A	-	-	-
18	A	245.98	-	245.98
19	A	36.25	-	36.25
20	CG	835.56	32.99	868.55
21	CG	216.28	37.23	253.52
22	CG	16.42	37.23	53.66
23	CG	11.10	37.23	48.34
24	W	-	1396.09	1396.09
25	W	8.09	1396.09	1404.19
26	W	0.17	26.12	26.28
27	W	0.20	26.12	26.31
28	W	9.90	26.12	36.01
29	W	8.96	28.82	37.78
30	W	11.30	29.48	40.78
31	W	12.44	29.48	41.91
32	W	6.74	2.63	9.37
33	W	49.90	19.48	69.39
34	S	118.45	19.48	137.93
35	S	4.01	0.66	4.67
36	S	165.88	26.12	191.99
37	S	202.25	26.12	228.37
38	S	218.51	26.12	244.62
39	S/W	13.84	26.12	39.96

A - air, W - water, Oxyg - oxygen, Syng - syngas, Slg - slag, AcGs - acid gas removal, CG - combustion gas, S - steam, S/W - steam–water mixture.

occurs at the condenser, the exergy analysis of this plant shows that only 1.04% of the total exergy is lost in the condenser. The lowest exergy efficiencies are calculated in pumps and heat exchangers. The total exergy destruction of the power plant is 692.59 MW, and the exergy efficiency of the overall power plant is 37.88%. The net electric efficiency of the simulated cycle, given in Table 1, is higher than the exergy efficiency of the power plant. It seems obvious from the data in Table 6 that irreversibility associated with chemical reactions is the main source of the exergy destruction. Furthermore, the exergy destruction of the gasifier and the combustion chamber should be decreased in order to increase the exergy efficiency of the IGCC.

4.3. Exergy analysis results of the IGCC operating with other Turkish lignite types

Figure 2 is a comparative summary of the exergy destruction and generated power data of the same simulated IGCC power plant, operating with different types of Turkish lignites. Characteristics of these lignites are given in Table 7. Power generation of all power plants are approximately equal, since the properties of the inlet and outlet streams of both gas and steam turbines are of the same value. These values directly affect the output power of the power plants.

Additionally, the maximum exergy destruction occurs in the Çan power plant with 1114 MW. The Yatağan and Çayırhan plants show values of 1017 and 1013 MW, respectively. The minimum exergy destructions occur at the Yeniköy and Soma plants with 692 and 721 MW, respectively.

Exergy efficiency of each plant is calculated with 2 distinct definitions and are shown in Figure 3. In the first approach, the exergy of production is defined as only the net power, but in the second, it is defined as net power plus exergy of the acid gas, which is a valuable by-product of an IGCC. Regarding the first definition, Yeniköy and Yatağan have the highest and lowest exergy efficiencies with 39.97% and 34.41%, respectively. When considering exergy with acid-gas, the highest and lowest second law efficiencies occur at Soma and Çan at 37.98% and 27.05%, respectively.

Table 6. Exergy destruction data and exergy efficiency of the Yeniköy power plant components.

Component	Exergy destruction	Dimensionless exergy destruction	Exergy efficiency
	(MW)	(%)	(%)
ASU	4.01	0.58	78.71
C. chamber	179.57	25.93	83.03
Compressor	11.44	1.65	96.10
Condenser	7.20	1.04	52.93
Deaerator	1.68	0.24	96.05
GCS	82.94	11.97	90.12
Gas turbine	37.90	5.47	94.18
Gasifier	320.25	46.24	65.10
Heat exchanger	2.83	0.41	46.91
HRSG	15.28	2.21	92.36
Pump1	2.55	0.37	30.82
Pump2	0.10	0.01	51.33
Pump3	0.10	0.01	45.99
Pump4	0.03	0.0001	50.16
Steam turbine	25.78	3.72	90.01
Valve	0.95	0.14	99.88
Overall plant	692.59	100.00	37.88

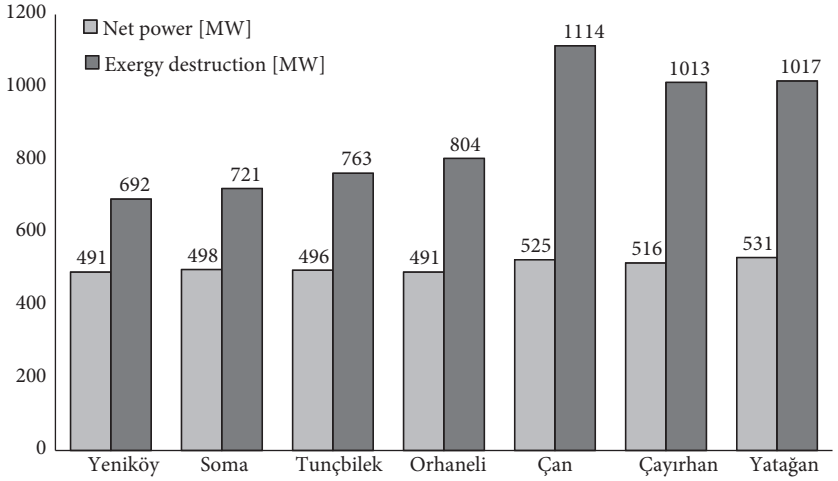

Figure 2. Exergy destruction rate and generated net power of the IGCC for all lignites used.

Table 7. Elemental analysis and lower heating values of the utilized lignites (data from General Directorate of Mineral Research and Exploration of Turkey, www.mta.gov.tr).

Locations	C	H	O	S	N	W	A	LHV
	(%)	(%)	(%)	(%)	(%)	(%)	(%)	(kJ/kg)
Yeniköy	39.05	3.02	11.21	1.42	1.46	24.26	19.58	14,626
Soma	38.64	2.74	16.40	0.01	0.59	18.64	22.98	13,455
Tunçbilek	42.52	2.84	12.68	1.98	0.98	27.38	11.62	14,734
Orhaneli	47.46	3.29	11.97	1.56	2.00	26.25	7.47	16,085
Çan	30.18	2.45	10.06	5.28	0.31	20.36	31.36	10,605
Çayırhan	31.68	2.58	7.81	2.49	1.23	24.69	29.52	11,156
Yatağan	29.16	2.55	12.68	1.85	0.27	31.17	22.32	10,254

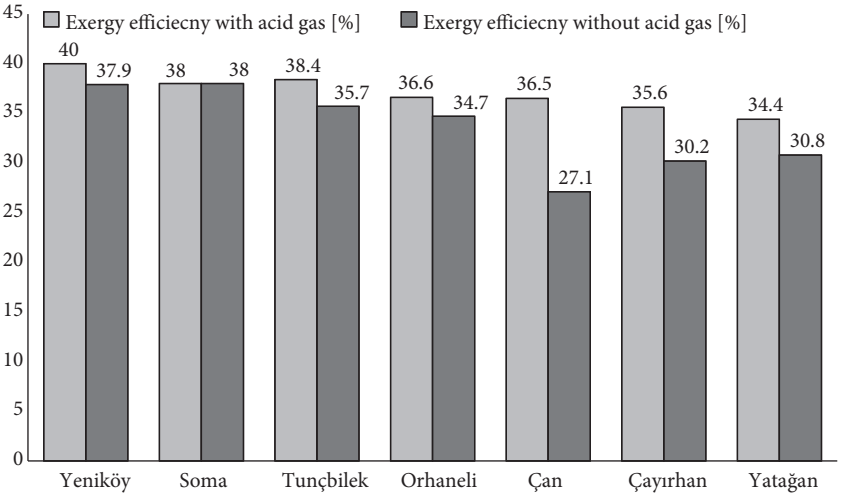

Figure 3. Exergy efficiency of the IGCC for all lignites used.

For a deeper insight into the conclusions, a summary of CO_2 emissions and feeding fuel rates of the IGCCs is presented in Figure 4. One can see that Çan and Yatağan have the maximum CO_2 emissions at 918 and 863 kg/s, respectively. The minimum CO_2 emission is at Yeniköy with a value of 726 kg/s.

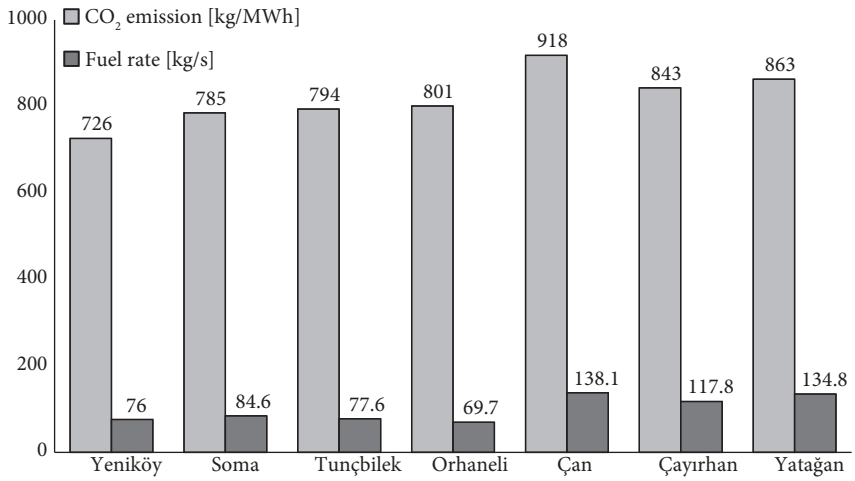

Figure 4. CO_2 emissions and feeding fuel rate of the different power plants.

5. Conclusions

In this study, energy and exergy analysis of an integrated gasification combined cycle was presented. The gasifier island consisted of a Texaco type gasifier. A one stage, slurry fed, oxygen blown, and cold gas cleaning system was applied. The Mitsubishi 701F type of gas turbine was selected for the simulations and the waste heat was utilized in a HRSG. The exergy destruction rates and exergy efficiencies of each component of the plant were evaluated. The analysis included 7 different Turkish lignite types. Fuel rates and CO_2 emission values of each case were also determined and compared. Several important results drawn from this study are summarized below.

- Total generated power of the Yeniköy lignite considered in this study as the base study was found to be 491 MW with net energy efficiency of 44.17%. Total exergy destruction and net exergy efficiency of the plant were 692 MW and 39.97%, respectively.
- Exergy analysis showed that the main exergy destruction took place in the gasifier at 320.25 MW and 46.24%.
- From the calculated exergy efficiency and CO_2 emissions, it can be stated that Yeniköy lignite is the best type among those considered for the same power generation capacity.
- Exergy is mostly destructed in the Çan and Yatağan lignite cases. The main reason for this could be seen in the elemental analysis of these lignites. Carbon and hydrogen percentages of these types are the lowest among the other types.

Nomenclature

e	Specific exergy (kJ/kg)
$\dot{E}$	Exergy rate (MW)
ε	Exergy efficiency (%)
h	Specific enthalpy (kJ/kg)
$\dot{m}$	Mass flow rate (kg/s)
P	Pressure (kPa)
$\dot{Q}$	Heat loss (MW)
s	Specific entropy (kJ/kg K)
T	Temperature (°C)
$\dot{W}$	Work rate (MW)

Subscripts

0	Dead state condition
ASU	Air separation unit
CH	Chemical
Comp.	Compressor
Cond.P.	Condenser pump
CV	Control volume
D	Destruction
i	Inlet
F	Fuel
Gas.	Gasifier

GCS	Gas cleanup system	*P*	Product
GT	Gas turbine	*PH*	Physical
KN	Kinetic	*PT*	Potential
o	Outlet	*ST*	Steam turbine

Appendix. Exergy formulas and efficiencies of each component.

Component	Exergy input	Exergy output	Work input/output	Exergy efficiency	
ASU	$\dot{E}_1 + \dot{E}_3$	$\dot{E}_5 + \dot{E}_4 + \dot{E}_6$	$\dot{W}_{A.S.U.}$	$\frac{\dot{E}_5+\dot{E}_6+(\dot{E}_3-\dot{E}_4)}{\dot{E}_1+\dot{W}_{A.S.U.}}$	
C. chamber	$\dot{E}_{16} + \dot{E}_{18}$	$\dot{E}_{20}$	-	$\frac{\dot{E}_{20}}{\dot{E}_{16}+\dot{E}_{18}}$	
Compressor	$\dot{E}_{17}$	$\dot{E}_{18} + \dot{E}_{19}$	$\dot{W}_{Comp.}$	$\frac{(\dot{E}_{18}+\dot{E}_{19})-\dot{E}_{17}}{\dot{W}_{Comp.}}$	
Condenser	$\dot{E}_{24} + \dot{E}_{39}$	$\dot{E}_{25} + \dot{E}_{26}$	$\dot{W}_{Cond.P.}$	$\frac{\dot{E}_{25}-\dot{E}_{24}}{\dot{E}_{39}-\dot{E}_{26}+\dot{W}_{Cond.P.}}$	
Deaerator	$\dot{E}_{29} + \dot{E}_{35}$	$\dot{E}_{30}$	-	$\frac{\dot{E}_{30}}{\dot{E}_{29}+\dot{E}_{35}}$	
GCS	$\dot{E}_8 + \dot{E}_{12} + \dot{E}_{27}$	$\dot{E}_{13} + \dot{E}_{14}$ $+\dot{E}_{15} + \dot{E}_{28}$	$\dot{W}_{G.C.S.}$	$\frac{\dot{E}_{13}+\dot{E}_{14}+\dot{E}_{15}+(\dot{E}_{28}-\dot{E}_{27})}{\dot{E}_8+\dot{E}_{12}+\dot{W}_{G.C.S.}}$	
Gas turbine	$\dot{E}_{19} + \dot{E}_{20}$	$\dot{E}_{21}$	$\dot{W}_{G.T.}$	$\frac{\dot{W}_{G.T.}}{\dot{E}_{19}+\dot{E}_{20}-\dot{E}_{21}}$	
Gasifier	$\dot{E}_6 + \dot{E}_7$ $+\dot{E}_{32} + \dot{E}_{33}$	$\dot{E}_8 + \dot{E}_9 + \dot{E}_{34}$	$\dot{W}_{Gas.}$	$\frac{\dot{E}_{18}+(\dot{E}_{33}-\dot{E}_{34})}{\dot{E}_6+\dot{E}_7+\dot{E}_{32}-\dot{E}_9+\dot{W}_{Gas.}}$	
Heat exchanger	$\dot{E}_{11} + \dot{E}_{22}$	$\dot{E}_{12} + \dot{E}_{23}$	-	$\frac{\dot{E}_{12}-\dot{E}_{11}}{\dot{E}_{22}-\dot{E}_{23}}$	
HRSG	$\dot{E}_{21} + \dot{E}_{31}$ $+\dot{E}_{34} + \dot{E}_{36}$	$\dot{E}_{22} + \dot{E}_{32}+$ $\dot{E}_{33} + \dot{E}_{35}+$ $\dot{E}_{37} + \dot{E}_{38}$	-	$\frac{(\dot{E}_{38}+\dot{E}_{32}+\dot{E}_{33}-\dot{E}_{31}-\dot{E}_{34})+(\dot{E}_{37}-\dot{E}_{36})}{\dot{E}_{21}-\dot{E}_{22}}$	
Pump1	$\dot{E}_{30}$	$\dot{E}_{31}$	$\dot{W}_{P.1}$	$\frac{\dot{E}_{31}-\dot{E}_{30}}{\dot{W}_{P.1}}$	
Pump2	$\dot{E}_2$	$\dot{E}_3$	$\dot{W}_{P.2}$	$\frac{\dot{E}_3-\dot{E}_2}{\dot{W}_{P.2}}$	
Pump3	$\dot{E}_{10}$	$\dot{E}_{11}$	$\dot{W}_{P.3}$	$\frac{\dot{E}_{11}-\dot{E}_{10}}{\dot{W}_{P.3}}$	
Pump4	$\dot{E}_{26}$	$\dot{E}_{27}$	$\dot{W}_{P.4}$	$\frac{\dot{E}_{27}-\dot{E}_{26}}{\dot{W}_{P.4}}$	
Steam turbine	$\dot{E}_{37} + \dot{E}_{38}$	$\dot{E}_{36} + \dot{E}_{39}$	$\dot{W}_{S.T.}$	$\frac{\dot{W}_{S.T.}}{\dot{E}_{37}-\dot{E}_{36}+\dot{E}_{38}-\dot{E}_{39}}$	
Valve	$\dot{E}_{15}$	$\dot{E}_{16}$		$\frac{\dot{E}_{16}}{\dot{E}_{15}}$	
Overall plant	$\dot{E}_1 + \dot{E}_2 + \dot{E}_7$ $+\dot{E}_{10} + \dot{E}_{17} + \dot{E}_{24}$	$\dot{E}4 + \dot{E}_9+$ $\dot{E}_{13} + \dot{E}_{14}+$ $\dot{E}_{23} + \dot{E}_{25}$	$\dot{W}_{net}$	With acid gas	Without acid gas
				$\frac{\dot{W}_{net}+\dot{E}_{14}}{\dot{E}_7}$	$\frac{\dot{W}_{net}}{\dot{E}_7}$

References

Ari, I. and Koksal, M.A., "Carbon Dioxide Emission from Turkish Electricity Sector and Its Mitigation Options, Energy Policy", 39, 6120–6135, 2011.

Bejan, A., Advanced Engineering Thermodynamics, John Wiley & Sons, Inc., New York, 1988.

Bejan, A., Tsatsaronis, G. and Moran, M., Thermal Design and Optimization, John Wiley & Sons, Inc., New York, 1996.

Chen, C. and Rubin, E., "CO_2 Control Technology Effects on IGCC Plant Performance and Cost", Energy Policy, 37, 915–924, 2009.

Coskun, C., Oktay, Z. and Dinçer, İ., "Investigation of Some Renewable Energy and Exergy Destruction Parameters for Two Geothermal District Heating Systems", International Journal of Exergy, 8, 1–15, 2011.

Decamps, C., Bouallou, C. and Kanniche, M., "Efficiency of an IGCC Power Plant Including CO_2 Removal", Energy, 33, 874–881, 2008.

Dincer, I. and Al-Muslim, H., "Energy and Exergy Efficiencies of Reheat Cycle Steam Power Plant", Proceedings of ECOS'01, İstanbul, 2001.

Duan, L., Lin, R., Deng, S., Jin, H. and Cai, R., "A Novel IGCC System with Steam Injected H_2/O_2 Cycle and CO_2 Recovery", Energy Conversion and Management, 45, 797–809, 2004.

Fortes, M., Bojarski, A.D., Velo, E., Nougues, J.M. and Puigjaner, L., "Conceptual Model and Evaluation of Generated Power and Emissions in an IGCC Plant", Energy, 34, 1721–1732, 2009.

Guillermo Ordorica-Garcia, G., Douglas, P., Croiset, E. and Zheng, L., "Technoeconomic Evaluation of IGCC Power Plants for CO_2 Avoidance", Energy Conversion and Management, 47, 2250–2259, 2006.

Huang, Y., Rezvani, S., Wright, D., Minchener, A. and Hewitt, N., "Techno-economic CO_2 Capture and Storage in Coal Fired Oxygen Fed Entrained Flow IGCC Power Plants", Fuel Processing Technology, 89, 916–925, 2008.

Jiang, L., Lin, R., Jin, H., Cai, R. and Liu, Z., "Study on Thermodynamic Characteristic and Optimization of Steam Cycle System in IGCC", Energy Conversion and Management, 43, 1339–1348, 2002.

Jimenez, L., Gadalla, M., Boer, D. and Majozi, T., "IGCC Process Simulation and Optimization", Computers and Chemical Engineering, 34, 331–338, 2010.

Kotas, T.J., The Exergy Method of Thermal Plant Analysis, Anchor Brendon Ltd., Tiptree, Essex, 1985.

Mondol, J.D., Wright, D., Rezvani, S., Huang, Y. and Hewitt, N., "Techno-economic Evaluation of Advanced IGCC Lignite Coal Fuelled Power Plants with CO_2 Capture", Fuel, 88, 2495–2506, 2009.

Oktay, Z., "Investigation of Coal-fired Power Plants in Turkey and a Case Study: Can Plant", Applied Thermal Engineering 29, 550–557, 2009.

Rezenbrink, W., Evers, J., Keller, D., Wolf, K.J. and Apel, W., "RWE's 450 MW IGCC/CCS Project-Status and Outlook", Energy Procedia 1, 615–622, 2009.

Zheng, L. and Furinsky, E., "Comparison of Shell, Texaco, BGL and KRW Gasifiers as a Part of IGCC Plant Computer Simulations", Energy Conversion and Management, 46, 1767–1779, 2005.